© 2018. Published by The Company of Biologists Ltd | Journal of Experimental Biology (2018) 221, jeb173369. doi:10.1242/jeb.173369

RESEARCH ARTICLE

Polarized object detection in crabs: a two-channel system

Melanie Ailín Basnak[1,2], Verónica Pérez-Schuster[1,3], Gabriela Hermitte[1] and Martín Berón de Astrada[1,*]

ABSTRACT

Many animal species take advantage of polarization vision for vital tasks such as orientation, communication and contrast enhancement. Previous studies have suggested that decapod crustaceans use a two-channel polarization system for contrast enhancement. Here, we characterize the polarization contrast sensitivity in a grapsid crab. We estimated the polarization contrast sensitivity of the animals by quantifying both their escape response and changes in heart rate when presented with polarized motion stimuli. The motion stimulus consisted of an expanding disk with an 82 deg polarization difference between the object and the background. More than 90% of animals responded by freezing or trying to avoid the polarized stimulus. In addition, we co-rotated the electric vector (e-vector) orientation of the light from the object and background by increments of 30 deg and found that the animals' escape response varied periodically with a 90 deg period. Maximum escape responses were obtained for object and background e-vectors near the vertical and horizontal orientations. Changes in cardiac response showed parallel results but also a minimum response when e-vectors of object and background were shifted by 45 deg with respect to the maxima. These results are consistent with an orthogonal receptor arrangement for the detection of polarized light, in which two channels are aligned with the vertical and horizontal orientations. It has been hypothesized that animals with object-based polarization vision rely on a two-channel detection system analogous to that of color processing in dichromats. Our results, obtained by systematically varying the e-vectors of object and background, provide strong empirical support for this theoretical model of polarized object detection.

KEY WORDS: Arthropod, Polarization, Vision

INTRODUCTION

Both vertebrates and invertebrates show sensitivity for the orientation of the electric vector (e-vector) of light (reviewed in Horváth and Varjú, 2004; Marshall and Cronin, 2011; Labhart, 2016). Polarization vision is a multi-purpose ability that has been shown to be involved in providing insects with a visual compass, the detection of water bodies in flying insects, visual communication in cephalopods, and enhancing object contrast in cephalopods and decapod crustaceans (Shashar and Cronin, 1996; Marshall et al., 2011; Wehner, 2001; Wehner and Labhart, 2006; Labhart, 2016). In particular, the usage of polarized light to enhance object or motion detection, termed object-based polarization vision, has gained significant attention in recent years (How and Marshall, 2014; Labhart, 2016). This visual ability has been recognized in a number of animals inhabiting intertidal and aquatic environments. In these environments, the animals would benefit from a horizontally polarized light field produced by reflections from horizontal surfaces or scattering from particles in the water column (Johnsen et al., 2011). Particularly, the benefits derived from sensing polarized light reflections on the ground would be greater in intertidal environments, where reflections provide a stronger horizontally polarized background than in aquatic environments (the change in refractive index between wet sand and air is higher than between sand and water).

The two groups of animals with the most outstanding object-based polarization vision studied so far, cephalopods and decapod crustaceans, discriminate linearly polarized light across broad regions of the visual field (Glantz, 2007; Talbot and Marshall, 2011; Alkaladi et al., 2013). Vision in both groups is mediated by rhabdomeric photoreceptors (Cronin et al., 2014). In these photoreceptors, rhodopsin is contained in finger-like microvilli that constrain its orientation. As rhodopsin is a dichroic photopigment and its distribution is spatially constrained, light becomes maximally absorbed when its e-vector is parallel to the long axis of the microvillus (reviewed in Roberts et al., 2011). In a polarization-sensitive photoreceptor, the microvilli are all oriented parallel to each other and, thus, the cell inherits the polarization sensitivity of the microvilli. In decapod crustaceans, the entire visual space is imaged by two groups of photoreceptors with orthogonal microvilli that are maximally sensitive to vertically or horizontally oriented e-vectors (Waterman, 1981; Alkaladi et al., 2013; but see Glantz, 2007).

The polarization sensitivity of photoreceptors in crayfishes and crabs has been studied with electrophysiological recordings (Waterman and Fernández, 1970; Shaw, 1969; Stowe, 1980). Crayfish photoreceptors were found to be sensitive exclusively to vertically or horizontally polarized light around the central pole of the eye, whereas photoreceptors with diagonal sensitivities were also found in the anterior, posterior and dorsal retina (Glantz, 2007). In crabs, less detailed studies have been performed; however, selective adaptation studies as well as intracellular recordings indicate there are mainly two families of polarization-sensitive photoreceptors that are maximally sensitive to vertically and horizontally polarized light (Waterman and Horch, 1966; Shaw, 1969; Waterman, 1981).

Laboratory-based studies have shown that crayfishes and crabs from the family Ocypodidae can use polarization information to detect apparent motion of looming figures (Tuthill and Johnsen, 2006; How et al., 2014). *Uca vomeris* crabs were found to be highly sensitive to polarized light, being able to detect stimuli differing in e-vector angle with respect to the background by just 3 deg (How et al., 2012). Moreover, it was shown that target detection is enhanced in fiddler crabs by polarization vision in their natural environment (How et al., 2015).

[1]Laboratorio de Neurobiología de la Memoria, Departamento de Fisiología, Biología Molecular y Celular, FCEyN, Universidad de Buenos Aires, IFIBYNE-CONICET, Buenos Aires, 1428, Argentina. [2]Department of Neurobiology, Harvard Medical School, Boston, MA 02115, USA. [3]Departamento de Física, FCEyN, Universidad de Buenos Aires, Buenos Aires, 1428, Argentina.

*Author for correspondence (martin@fbmc.fcen.uba.ar)

Received 2 November 2017; Accepted 10 April 2018

Journal of Experimental Biology (2018) 221, jeb173369. doi:10.1242/jeb.173369

Based on the pioneering work of Bernard and Wehner (1977), a general theoretical model for estimating the discriminability of polarized objects was proposed recently (How and Marshall, 2014). According to this model, in a horizontally polarized light field, a two-channel sensitive system with maximal polarization sensitivity in the horizontal and vertical directions is optimally designed for detecting objects based on the degree of polarization contrast between object and background (How and Marshall, 2014). In spite of the apparent generality and predictive power of the model (see Discussion), empirical evidence supporting it is scant (How et al., 2014).

With the main goal of evaluating the model for estimating the discriminability of polarized objects, here, we confronted the grapsid crab *Neohelice granulata* with looming disks that differed from the background in only the e-vector of light. To determine whether *N. granulata* has a preference for certain e-vector orientations, we used stimuli with a constant angular difference between the e-vectors from the object and the background, but systematically co-varied their orientation with respect to the vertical. We estimated the polarization sensitivity of the animals by quantifying their escape behavior and changes in their heart rate, a remarkably sensitive variable of the animal's internal state (e.g. Beauchamp and Rowe, 1977; Grober, 1990). A 90 deg periodic function fits the animals' responses, with maximum responses for object and background e-vectors aligned with the vertical and horizontal orientations. These results suggest that *N. granulata* possesses object-based polarization vision mediated by two orthogonal channels aligned with the vertical and horizontal axes. The periodicity of orientation sensitivity found in our crab model is in close agreement with that predicted by the theoretical model for polarized object detection, providing strong empirical support for it (see Discussion).

MATERIALS AND METHODS

Animals

Adult male *Neohelice granulata* (Dana 1851) crabs (previously *Chasmagnathus granulatus*; Sakai et al., 2006) were used in the present study. *Neohelice granulata* inhabits densely vegetated mudflats in the upper intertidal zone. Animals 2.7–3.0 cm across the carapace, weighing approximately 17 g, were collected from the beaches of San Clemente del Tuyú, Argentina. They were transported to the laboratory at the Universidad de Buenos Aires and kept in rectangular plastic tanks (35×48×27 cm) filled to a 0.5 cm depth with marine water prepared using hw-Marinex (Winex-Germany, Hamburg, Germany) (salinity 10–14‰, pH 7.4–7.6). The holding and experimental rooms were maintained on a 12 h:12 h light:dark cycle (lights on: 07:00–19:00 h) at 22–24°C. Measurements were carried out between 07:00 and 19:00 h in the first 2 weeks following the animals' arrival to the laboratory. All experimental protocols were performed in accordance with relevant guidelines and ethical regulations of the School of Science, Universidad de Buenos Aires.

Polarized light stimuli

In order to generate polarization stimuli, the outer-most polarizing filter of a liquid crystal display (LCD; Samsung SyncMaster SA300, Seoul, Republic of Korea) was removed (Glantz and Schroeter, 2006; Pignatelli et al., 2011; Temple et al., 2012). By varying the grayscale values of the modified monitor, this yielded polarized light images which allowed us to create stimuli with e-vector contrast but no intensity or spectral contrast. From 0 to 255 in the grayscale, the modified screen appeared as a homogeneously back-lit surface to the human eye, but displayed polarized light emissions. The angle between the e-vectors of two such emissions could be as wide as 82 deg (RGB: 0, 0, 0 versus RGB: 255, 255, 255). To calibrate our modified LCD screen, we used the Stokes parameters, indices that allow us to characterize the polarization of light (Johnsen, 2012). To this end, we used a visible linear polarizing laminated film (Edmund Optics Ltd, York, UK) mounted on a rotary mount. All light measurements were performed with the irradiance sensor (J1812) of a Tektronix J17 photometer (Wilsonville, OR, USA). Fig. 1C shows the general calibration of our monitor screen, which produced a profile of polarized light emissions highly similar to those of previously described LCD displays used in similar experiments (e.g. Glantz and Schroeter, 2006; How et al., 2012).

We stimulated the animals with a looming disk of grayscale value 255 (RGB: 255, 255, 255) expanding over a homogeneous background of 0 (RGB: 0, 0, 0). The angular difference between the object and background e-vectors was 82 deg. The degree of linear polarization, i.e. the intensity of linearly polarized light with respect to the total amount of light, was 0.84 for the object and 0.97 for the background. The change in intensity between object and background at full size was 0.4% of total light intensity, a value similar to that obtained in previous studies (How et al., 2012; Temple et al., 2012).

The looming disk was centered at the monitor's midpoint and simulated a spherical object of 35.5 cm in diameter approaching the crab over a distance of 5 m at a constant speed of 146.6 cm s^{-1}. The object subtended an angle of 4 deg at its stationary initial position and expanded up to 60 deg in 3.2 s. Previous studies have used this stimulus to provoke an escape response in *N. granulata* (Oliva et al., 2007; Oliva and Tomsic, 2012).

The modified LCD was mounted on a spinning support that allowed us to rotate it around its center. Throughout these experiments, we presented the same object expanding over the same background. By rotating the support, the e-vector of both object and background shifted together. In our reference system, 0 deg corresponds to the vertical orientation. In the experiments in which we quantified the escape response, seven polarization stimuli spanning 180 deg were generated every 30 deg, and denoted 0, 30, 60, 90, 120, 150 and 180 deg according to the background e-vector orientation. In the electrocardiogram (ECG) experiments in which we measured the animals' heart rate, we generated five stimuli spanning 90 deg every 22.5 deg. Using the same criterion, these stimuli were named 0, 22.5, 45, 67.5 and 90 deg.

In both the behavioral and physiological experiments, a black foam mask with the diameter of the maximal size reached by the looming disk carved in it was positioned in front of the monitor (Fig. 1A,B). This corrected for visual asymmetries for different rotation angles of the screen.

Escape response

Animals were placed on a 40×40 cm walking simulator device enclosed by two screens, the modified LCD and a cathode ray tube (CRT) monitor on the opposite side (Philips 107T CRT, Suzhou, China; refresh rate 60 Hz), each one located 20 cm away from the animal. The two remaining sides were covered with white foam boards, also 20 cm away (Fig. 1A). To avoid asymmetric lighting of the behavioral setup, the CRT monitor showed a homogeneous white emission, with a brightness similar to that of the modified LCD.

The walking simulator device consisted of a 16 cm diameter Styrofoam ball floating on water that could be freely rotated by the

Journal of Experimental Biology (2018) 221, jeb173369. doi:10.1242/jeb.173369

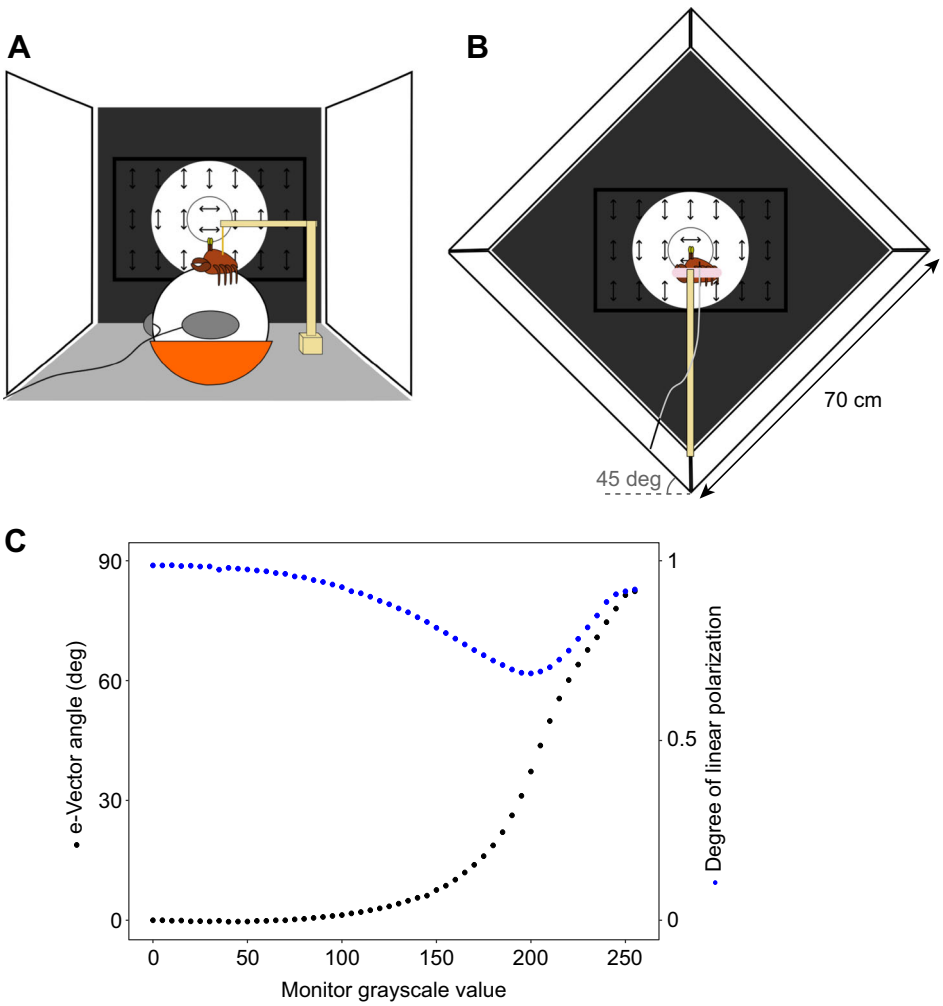

Fig. 1. Experimental setups and monitor calibration. (A) Experimental setup to quantify the animal's escape response, illustrated slightly from above. The crab was held on top of a Styrofoam ball floating on water, where it could move its legs freely. Circular looming stimuli were presented on an LCD, modified to produce polarized emissions (at the back). The screen was free to rotate to change the e-vector angle of light from the object and the background. The rotation angle of the monitor illustrated corresponds to the stimulus denoted 0 deg [background vertically polarized (0 deg) and object horizontally polarized (82 deg)]. A black foam mask was placed in front of the screen, covering everything except a disk of the maximal size reached by the object. Thus, the different stimuli were equivalent in terms of form. The opaque mask is shown with some transparency here for clarity. Two PC optical mice recorded the animal's position in *x* and *y* coordinates. (B) Experimental setup to study the cardiac activity. The crab was held fixed with an adjustable clamp, and its claws and legs were secured against its body with a rubber band. The same stimulation monitor was used, but it was placed at the end of a white box with its walls at 45 deg from the vertical.
(C) Polarization properties of the modified LCD. Varying the grayscale value of the emissions results in a change in the e-vector angle (black circles) as well as a change in the degree of linear polarization (blue circles). It is worth noting that only the first and last values of the grayscale were used in the present work.

animal from a standing position. A weightless rod was fixed to the crab's carapace with cyanoacrylate glue and placed into a guide to avoid rotational movements. In this setup, the animals could adopt their natural locomotion position and freely move their legs, rotating the sphere beneath them. The *x* and *y* coordinates of the sphere were recorded with two position sensors (optic PC mice; Genius GM-04003P, Taipei, Taiwan) every 16.7 ms, so that the attempted translational movements of the crabs could be reconstructed (Oliva et al., 2007). The crabs were positioned with the lateral pole of one of their eyes looking at the center of the modified LCD screen. Commercial software was used to deliver the visual stimuli and record the position of the Styrofoam ball (Presentation 5.3, Neurobehavioral Systems Inc., Albany, CA, USA). From the data recorded, we calculated: (1) the instantaneous velocity of the animals in cm s^{-1}, (2) the distance traveled during the visual stimulation, (3) the trajectories of movement and (4) the escape direction. The latter was calculated as the angle between the segment that links the initial and final apparent positions of the animal and the normal vector to the center of the stimulation monitor.

For qualitative analysis of their response, animals were filmed using a digital video camera (Shark Net, Sn W601). The behaviors were divided into four categories: (1) 'avoidance' – the animal walked or ran trying to evade the approaching object; (2) 'freezing' – the animal stopped moving when visually stimulated; (3) 'lateral merus display' – the animal raised its claws in the direction of the stimulus; and (4) 'no response'– the animal did not change its activity when the stimulus was presented.

Protocol

The crabs (n=226) were placed on the walking simulator and left visually undisturbed for 10 min, with the object at its initial size already present on the modified screen. Each animal was presented with one of the seven stimuli defined previously. The assignment of the animals to the experimental groups was randomized and an independent group of animals was assigned to a control group presented with a depolarized visual stimulus. The animals from the control group were stimulated with the monitor in the 0 deg position (background light vertically polarized). Wax paper was placed over the screen to depolarize the image (Tuthill and Johnsen, 2006). This resulted in a 35.8% reduction in light intensity, but effectively eliminated the polarization (the degree of linear polarization was less than 0.001 for emissions at RGB: 0, 0, 0 and RGB: 255, 255, 255).

Cardiac activity

A small jack, with two metallic pins where the electrodes were soldered, was cemented with cyanoacrylate glue to the dorsal carapace of the crabs just above the heart. The electrodes were made of silver wire (diameter 0.25 mm, VEGA & CAMJI S.A., Buenos Aires, Argentina). The free ends of both silver wires were inserted in holes drilled 4–5 mm apart in the cardiac region of the dorsal

carapace and cemented in place. All recording experiments were conducted at least 2 days after electrode positioning. To monitor the heart rate (f_H), the metallic pins were connected to an impedance converter (UFI, model 2991, Morro Bay, CA, USA). The impedance converter allowed recording the crab's f_H as a measure of dynamic resistance (Burnovicz et al., 2009; Yang et al., 2013). Its output was digitized (Digidata 1440A, Molecular Devices, Sunnyvale, CA, USA) and acquired with compatible software (AxoScope 10, Molecular Devices).

To quantify the cardiac activity, the period between two heart beats was measured and normalized to the mean period during 10 s prior to the stimulation. In this way, we obtained a temporal profile of the relative period of heart beats. We performed a linear interpolation between every two consecutive relative periods and integrated the area under the curve during the stimulation time plus 0.5 s after it. To reduce the inter-individual variations and the number of experimental subjects, we presented more than one stimulus to each animal. For each experimental group, we normalized the integrated cardiac response to each stimulus to the animal's total response (i.e. the sum of all the integrated responses to the individual stimuli). We used this variable, the normalized cardiac response, to compare the responses to the different visual stimuli (see Data analysis).

When illuminating a flat surface with linearly polarized light, the total amount of reflected light varies with the angle of polarization of the incident light (Johnsen, 2012). Almost all of the surfaces surrounding the animal in the setup for recording its escape response were vertical and horizontal (Fig. 1A). In such a surrounding, the changes in the intensity of the reflected light become maximal when the illumination shifts from horizontal to vertical and vice versa (e.g. with the stimuli denoted 0, 90 and 180 deg). Thus, even when this variation in the intensity of the reflected light is hardly noticeable, it could influence animal response. To avoid a possible bias in the stimulation, we modified the flanking surfaces of the animal to perform the f_H recordings. We built a box that consisted of four white foam-board walls, 100×70 cm each, placed at 45 deg from the vertical (Fig. 1B). In such a surrounding, we could not detect any change in the intensity of the reflected light when the illumination shifted from horizontal to vertical (or vice versa). Now, hardly noticeably changes in the intensity of the reflected light take place when changing illumination from 45 to −45 deg and vice versa. The modified LCD was placed at one end of the box. Each animal was held immobilized by an adjustable clamp, and placed at the center of the box, 20 cm away from the screen, with the lateral pole of the eye looking at its midpoint.

Protocol

The crabs were placed in the recording setup and left visually undisturbed for 10 min prior to the first trial presentation. The intertrial interval was 10 min. Two experiments were carried out with the ECG technique. The first was aimed at assessing whether the heart rate varies according to stimulus contrast. To this purpose, an unmodified LCD display was used (LG 32LA613B, LG Electronics, Seoul, Republic of Korea). We presented each crab (n=17) with five looming stimuli (a 27 cm spherical object approaching the crab over a distance of 4 m at a constant speed of 71.5 cm s^{-1}; the object subtended an angle of 4 deg at its stationary initial position and expanded up to 50 deg in 5.1 s). In this experiment, the background was always white (grayscale=255) and the object had different intensities (grayscale=235, 205, 165, 120 and 0). This resulted in five different intensity contrasts (0.10, 0.24, 0.42, 0.63 and 0.96, respectively, calculated with Michelson's equation). The sequence of stimuli presented to each animal was randomized.

The second experiment aimed to study the response to a 45 deg stimulus (background e-vector=45 deg) and was carried out using the modified LCD and looming stimulus described previously. Because there is some habituation of the heart rate response with the repeated visual stimulation (not shown), the animals were divided into two groups. One group received the stimuli with the monitor positioned at 0, 22.5 and 45 deg (n=13) and the other at 45, 67.5 and 90 deg (n=19) in a pseudorandom order.

Data analysis

Data analysis was conducted in R-Studio (version 3.3.1, CRAN, 2016). The difference between the distance traveled by the animals from the polarized 0 deg group and those from the depolarized control group was assessed with a Wilcoxon rank-sum test. Deviations from random distributions in the directions adopted during exploratory activity and expansion of the looming stimulus were evaluated using the Rayleigh test for circular statistics. The function $y=A\cos(\omega x+\phi)+B$ was fitted to the distances traveled by the animals in response to the seven polarization stimuli, where y is the distance and x is the e-vector angle of the background. We chose the distance traveled by the animals as a measure of the strength of the response to the polarized stimuli because the great majority of the animals increased their locomotor activity when confronted with the stimuli (Figs 2A and 3B,C). Moreover, in experiments in which animal avoidance was evoked by stimuli with varying intensity contrast, the distance traveled by the animals was strongly correlated with the intensity contrast of the moving object (collision trajectories: Oliva, 2010; translatory trajectories: Bengochea, 2017). The function was fitted to the individual data (n=226) by nonlinear least squares.

Heart rate experiments were analyzed using generalized linear mixed models with the statistical packages 'nlme' and 'multcomp', setting the stimulus' property (i.e. intensity contrast or e-vector angle) as a fixed factor and the animal as a random factor.

RESULTS

Animal behavior

Crabs faced with a polarized looming stimulus increased their locomotor activity as the object expanded. When the disk reached its maximal size, the instantaneous velocity of the animals started to decrease. The red curve in Fig. 2A shows the temporal profile of the response from an experimental group stimulated with a disk of horizontally polarized light (82 deg) expanding against a vertically polarized background (0 deg). As a control, the same stimulus was presented to an independent group of animals with wax paper placed over the screen to depolarize the image (Tuthill and Johnsen, 2006). The depolarized stimulus did not evoke any clear response (Fig. 2A, gray curve). The total distance traveled by the crabs during the expansion of the polarized stimulus was significantly higher than the distance traveled for the depolarized stimulus (experimental group=9.9 cm, n=33; control group=3 cm, n=15; P=0.002, Wilcoxon rank-sum test).

Even when most animals responded by evading the polarized looming disk, only in a few cases did this response consist of an intense run. However, regardless of the magnitude of the animal's response, the locomotor activity evoked by the stimulus had a similar profile (Fig. 2B). The trajectory adopted during the escape was also consistent across animals: they moved in the opposite direction of the approach of the stimulus (Fig. 2C, top), irrespective of the direction in which they were walking before the stimulation

Journal of Experimental Biology (2018) 221, jeb173369. doi:10.1242/jeb.173369

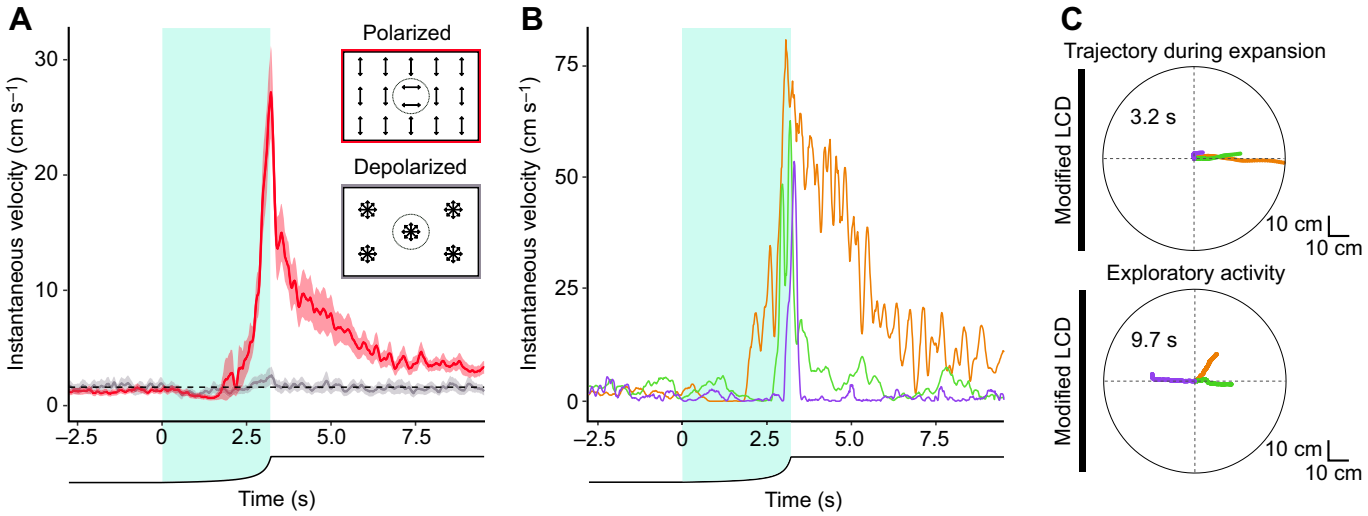

Fig. 2. Behavioral response to a polarized stimulus. (A) Instantaneous velocity (means±s.e.m.) of the animals when faced with a polarized stimulus (red line, n=33) and a depolarized stimulus (gray line, n=15). The dashed line represents the mean basal velocity during the 2.5 s prior to the stimulation. The black line under the plot illustrates the angular size of the looming object. The shaded area highlights the expansion of the object. (B) Individual responses of three animals to the polarized stimulus. (C) The traces illustrate the trajectories adopted by the same three animals during the 3.2 s of expansion (top) and during the 9.7 s prior to the stimulation (bottom). The black vertical line to the left represents the modified LCD seen from above. The polarized stimulus responses illustrated here correspond to a monitor rotation of 0 deg, i.e. object horizontally polarized (82 deg) and background vertically polarized (0 deg).

(Fig. 2C, bottom). Both the temporal profile of the response and the escape direction of the animals are in agreement with previous studies assessing the behavioral response of crabs to intensity-based looming objects (e.g. Oliva et al., 2007; Hemmi and Tomsic, 2012).

Our next step was to evaluate *N. granulata*'s sensitivity to the angles of polarization from the object and the background. In decapods, the polarization-sensitive photoreceptors seem to be arranged in such a way as to form two orthogonal channels. We thus designed our polarization stimuli to provoke different activation levels of such putative polarization channels. We stimulated the animals with a constant polarization difference between the e-vectors of the object and the background (82 deg, see Materials and methods), but varied the angle with which both e-vectors reached the eyes by rotating the modified LCD screen. We presented seven stimuli that were denoted according to the background e-vector: 0, 30, 60, 90, 120, 150 and 180 deg (the object e-vector being: 82, 112, 142, 172, 202, 232 and 262 deg, respectively). We expected the polarized looming stimulus to be perceived with maximal contrast when the background maximally activated one polarization channel and the object maximally activated the other.

A qualitative analysis of the behavior of the crabs showed that irrespective of the angles of stimulation, most animals responded, i.e. changed their behavior in some way, to the polarized looming disk (210 out of 226 crabs). The percentage of responding animals for each stimulus suggests that they are more likely to respond when the object and background e-vectors are vertical or horizontal (Fig. 3A). We classified the different behavioral responses as: (1) avoidance, (2) freezing and (3) lateral merus display (Fig. 3B). Out of the 210 animals that responded, only four did so by raising their claws, 16 animals froze and 190 avoided the approaching object, by far the most frequent behavior. We observed no clear differences in the distribution of the behaviors across stimuli.

Using the information from the walking simulator device, we could reconstruct animals' trajectories during the object's expansion for most of the animals that responded by moving. As shown in Fig. 2C, crabs consistently walked or ran in the opposite direction to that of the approaching disk (mean direction=181.1±4.6 deg, n=179, P<0.001, Rayleigh test; Fig. 3C, top), whereas the exploratory activity for those that were moving before the stimulation was randomly distributed (n=85, P=0.485, Rayleigh test; Fig. 3C, bottom).

We compared the response to the seven stimuli by quantifying the distance traveled during the disk's expansion (Fig. 3D). A cursory inspection of the results suggested that the escape distance was larger when the e-vectors of the object and the background were vertically or horizontally oriented. As the absorption of linearly polarized light by the dichroic rhabdomeres should roughly follow a periodic function (Waterman, 1981), and the determination of visual contrast would imply some comparison of at least two kinds of such inputs, which is also expected to be periodic (see Discussion; Bernard and Wehner, 1977; How and Marshall, 2014), we fitted a periodic function to the data to statistically evaluate the results. We used the function $y=A\cos(\omega x+\phi)+B$, where y is the distance traveled during the expansion of the stimulus and x is the rotation angle of the stimulation device. We obtained the best fit with the equation $y=2.93\cos(3.86x+0.14)+10.05$ (black curve in Fig. 3D). The estimated values for A and ω were significantly different from zero (A=2.93 cm, P=0.002, t-test; ω=3.86, $P=4.28e^{-14}$, t-test), which confirms a periodic modulation of the animals' escape response. As a control of this analysis, we fitted the same equation to a shuffled version of the data (we assigned each escape response to one of the seven stimuli randomly). The estimated value for A was not significantly different from zero (A=1.60 cm, P=0.140, t-test), indicating that a periodic function does not fit a randomized distribution of the data. In addition, we fitted a periodic function with a 180 deg period (ω=2) peaking for the vertical background (ϕ=0) to the data. The estimated value for A was also not significantly different from zero (A=1.35 cm, P=0.16, t-test), indicating that the data do not present a 180 deg periodicity. Finally, log transforming the data produced equivalent results for the different fits performed on the original data (analysis not shown).

To summarize, the fitted function to the real data has a period close to 90 deg (ω=3.86±0.94), with maximal responses for the stimuli we designated 0, 90 and 180 deg (ϕ=0.14, P=0.866, t-test).

Journal of Experimental Biology (2018) 221, jeb173369. doi:10.1242/jeb.173369

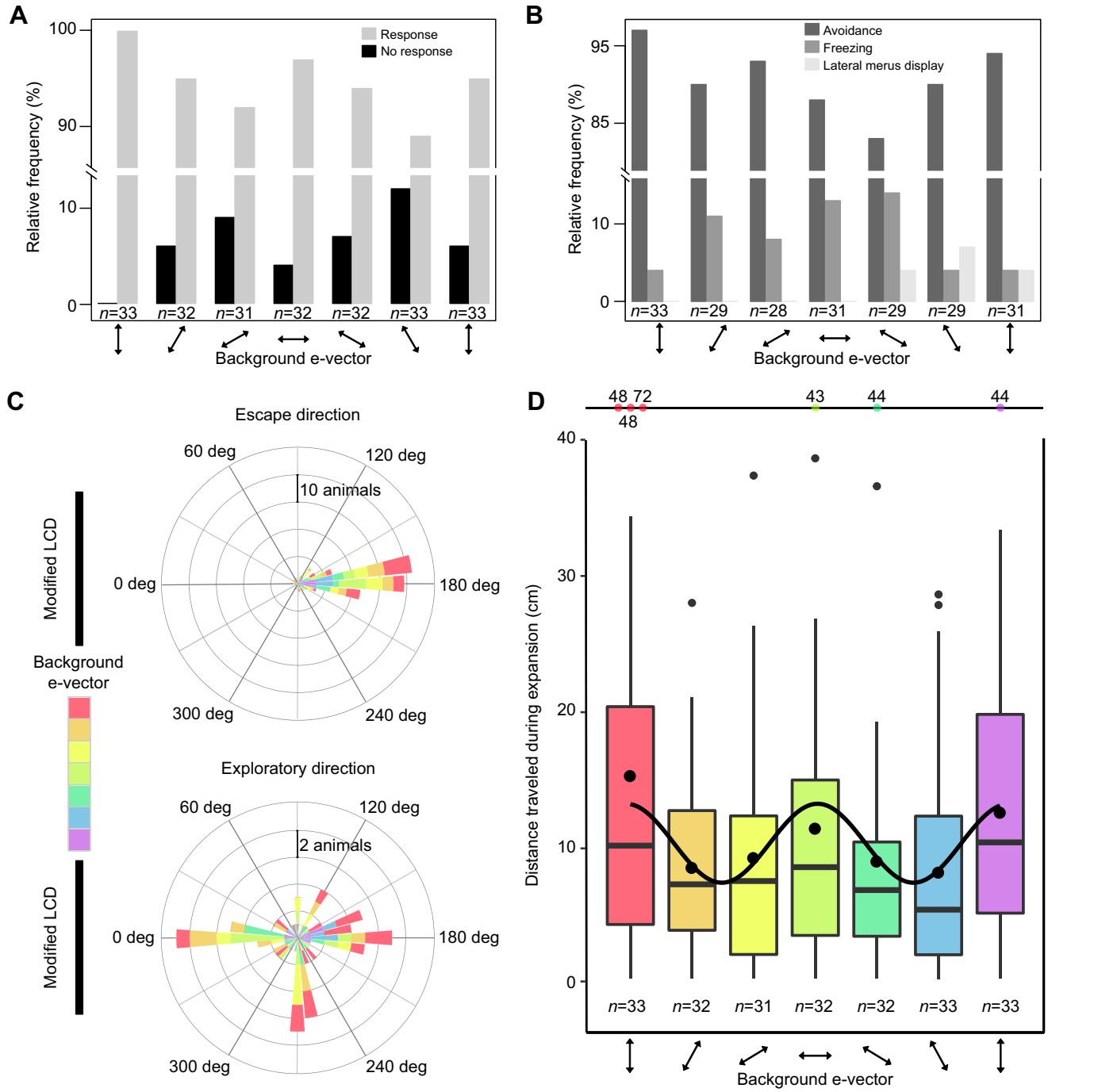

Fig. 3. Behavioral responses to the different polarized stimuli. (A) Percentages of animals that did and did not respond to the different polarized stimuli. The rotation angle of the monitor corresponds to the background e-vector orientation (arrows below the plots). From left to right, the background e-vectors are: 0, 30, 60, 90, 120, 150 and 180 deg; and the object e-vectors are: 82, 112, 142, 172, 202, 232 and 262 deg, respectively. (B) Percentages of animals, out of those that responded, displaying the three different behaviors defined qualitatively for each polarized stimulus. (C) Circular histograms illustrating the direction adopted by the animals during disk expansion (3.2 s, top; n=179) and exploratory activity (9.7 s, bottom; n=85). Bins of 10 deg were used in these plots. (D) Boxplots depicting the distance traveled during the expansion for the different polarization stimuli. The black circles indicate the mean distance traveled for each stimulus. Each colored circle at the top of the plot represents an outlier (its value is shown). The black curve represents the fit of the function y=2.93cos(3.86x+0.14)+10.05 to the data from the 226 animals. The sample size (n) for each experimental group in A, B and D is indicated in the figure.

For a 0 deg monitor rotation, the object is roughly horizontally polarized (e-vector 82 deg) and the background is vertically polarized (e-vector 0 deg); for a 90 deg rotation, the object is vertically polarized (e-vector 172 deg) and the background is horizontally polarized (e-vector 90 deg); and for a 180 deg rotation, the configuration is equivalent to that for 0 deg. Thus, *N. granulata* effectively seems to possess two polarization channels aligned with the vertical and horizontal.

Heart rate analysis

Animals could have remained behaviorally unaltered despite being internally excited. Thus, we decided to repeat these experiments

monitoring f_H, a widely used methodology in animals across many taxonomic groups as an indicator of internal state and sensory perception (e.g. Sand and Karlsen, 1986; Grober, 1990; King and Adamo, 2006). Our previous experiment predicts a function minimum for a rotation angle of the monitor close to 45 and 135 deg. To confirm there is a minimum for those angles, and not a local maximum, for example, we stimulated the animals with the same device and looming stimulus but included the 45 deg orientation. As a refinement of our first experiment, we reduced and shifted by 45 deg the putative influence of light reflections by placing the animals further away from the walls and rotating them by 45 deg (Fig. 1B and Materials and methods).

In *N. granulata*, bradycardia and heart arrest have been used before as a measure of the perception of mechanical and visual stimuli (e.g. Burnovicz et al., 2009; Yang et al., 2013). Here, we first tested whether changes in f_H can reflect the intensity contrast experienced by the animals. We recorded the f_H while exposing each crab to a pseudo-randomized sequence of five looming stimuli with different intensity contrasts. Fig. 4A illustrates the f_H of a representative animal when confronted with different contrast stimuli. The visual stimulation evoked a heart arrest, an increase in the heart rate period. Fig. 4B shows the analysis performed on the f_H recordings, in particular those of the animal in Fig. 4A. The f_H periods were measured and normalized to the mean period corresponding to 10 s before the stimulation (circular markers in Fig. 4B). The relative periods between beats were linearly interpolated (lines linking markers in Fig. 4B), obtaining a continuous temporal profile of the response for all the animals used. Both individually and on average, there was an increase in the response as the disk expanded, and then a rapid decrease after the object reached its maximal size (Fig. 4B,C). The magnitude of the response varied with the intensity contrast, with a higher contrast leading to a larger response. We quantified the cardiac response by calculating the area under the curve during the object's expansion, and normalized each response to the sum of the animal's responses to the different stimuli (Fig. 4D). The results obtained show that the f_H exhibits a graded response to stimulus intensity contrast (a second degree polynomial function properly fits the data: n=17; y=0.30x^2+0.01x+0.10, P<0.0001, linear mixed-effects model; dashed line in Fig. 4D).

These results show that the f_H period is a sensitive index of the contrast experienced by the animals. Using the looming stimulus with polarization-only contrast, we next studied whether there is a minimal response to a 45 deg rotation of the modified LCD screen. In order to reduce the number of animals used, we chose to assess only one period: from 0 to 90 deg. Thirteen animals received the stimuli 0, 22.5 and 45 deg (object e-vector: 82, 104.5 and 127 deg, respectively), whereas 19 received the stimuli 45, 67.5 and 90 deg (object e-vector: 127, 149.5 and 172 deg, respectively), both groups in a random sequence. Fig. 4E illustrates the f_H recordings from a representative crab when confronted with the stimuli 0, 22.5 and 45 deg (top, middle and bottom traces, respectively). The averaged temporal profile of the response was highly similar to that of the intensity contrast stimuli (not shown). Fig. 4F shows the normalized cardiac response during the expansion of the disk for the different stimuli. We found that for both groups of animals, the response was minimal for 45 deg (P=0.010 for 0 and 22.5 deg versus 45 deg; P=0.0005 for 67.5 and 90 deg versus 45 deg, linear mixed-effects model). These results show that, as with escape behavior, cardiac activity shows a maximal response when object and background e-vectors are aligned with the vertical and horizontal, and confirm a minimum response for a rotation of 45 deg.

DISCUSSION

The theoretical framework for predicting the visual contrast available for object detection in polarization scenes is based on color vision models (Bernard and Wehner, 1977). It proposes that the angle and degree of polarization, as parameters for a polarization vision system, are analogous to the dominant wavelength and purity, respectively, as parameters for a color vision system (e.g. completely linearly polarized light and unpolarized light are analogous to monochromatic light and white light, respectively). According to the model, a polarization vision system based on two independent channels is characterized by neutral points and confusion states of polarization comparable to a dichromatic color vision system. Recently, in consequence of the discovery of some animals using polarization information for detecting object motion based only on polarization information, the model was further extended (How and Marshall, 2014). In this last version, the polarization sensitivity of a photoreceptor (R) was modeled by the following equation:

$$R(\phi, d) = \left[1 + \left(\frac{d(S_p - 1)}{S_p + 1}\right)\right]\cos(2\phi - 2\phi_{max}), \quad (1)$$

where ϕ is the e-vector axis, d is the degree of linear polarization, ϕ_{max} is the orientation to which the polarization sensitivity of the photoreceptor is maximal and S_p is the level of effective polarization sensitivity of each photoreceptor (How and Marshall, 2014). S_p is calculated as the maximal sensitivity of the photoreceptor divided by its minimum sensitivity (Bernard and Wehner, 1977). In a two-channel system, the inputs from the two types of photoreceptors (R_1 and R_2) are combined in an opponent way in a first level interneuron (P):

$$P = \ln\left(\frac{R_1}{R_2}\right). \quad (2)$$

To extract the information about polarization contrast, the activity of two interneurons, one viewing the object (P_{obj}) and one the background (P_{bgd}), must be combined in a second order interneuron. The authors (How and Marshall, 2014) proposed a measure that models the difference in activity between the interneurons, the polarization distance (D_P):

$$D_P(\text{obj}, \text{bgd}) = \left|\frac{P_{obj} - P_{bgd}}{2\ln(S_p)}\right|. \quad (3)$$

According to the model, the highest contrast available ($D_P \approx 1$) to a two-channel system occurs when the object and background are fully linearly polarized with orthogonal e-vector axes matching the orientations of the two receptors. When linearly polarized light is midway between the two ϕ_{max} (i.e. ϕ_{max}±45 deg), signals from each photoreceptor population are identical, and these two angles are termed 'null points' or 'confusion points'. Thus, when linearly polarized light from the object and background match the orientations ϕ_{max}±45 deg, minimum responses are predicted.

In a previous study performed in another crab, *Uca heteropleura* (Ocypodidae), the animals were confronted with looming stimuli of increasing degree of linear polarization under two different alignment conditions of the background e-vector: aligned with the horizontal or aligned at 45 deg (How et al., 2014). *Uca heteropleura* was less sensitive to differences in the degree of polarized light when presented at 45 deg than when aligned with the horizontal. This result was interpreted as a strong indication of a behavioral null point in polarization sensitivity, a prediction of the theoretical framework for interpreting polarization sensitivity contrast. Aside

Journal of Experimental Biology (2018) 221, jeb173369. doi:10.1242/jeb.173369

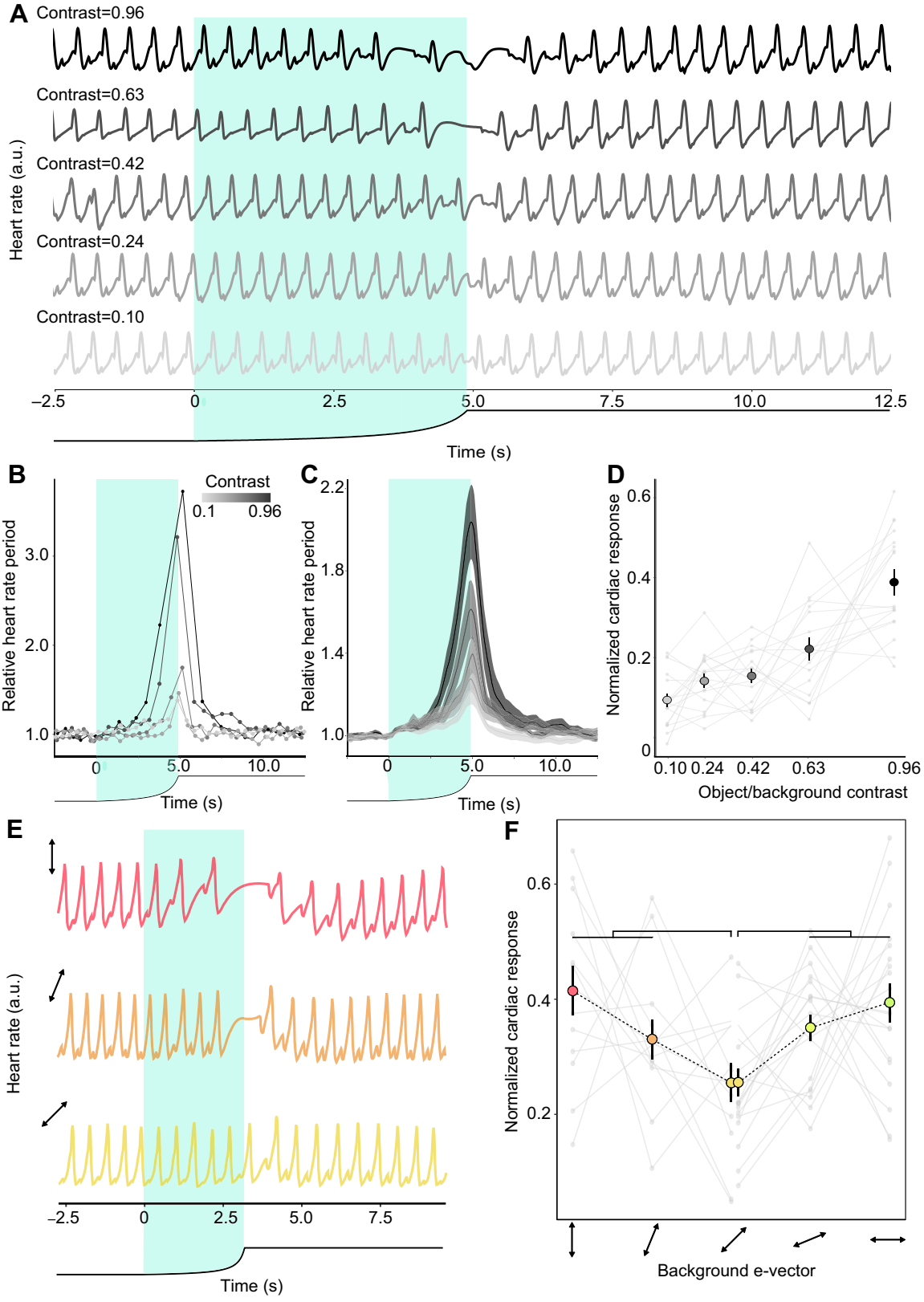

Fig. 4. See next page for legend.

Journal of Experimental Biology (2018) 221, jeb173369. doi:10.1242/jeb.173369

Fig. 4. Cardiac responses to intensity and polarization stimuli. (A) Heart rate (f_H) recordings from the same animal to five stimuli with different intensity contrasts. Increasing levels of gray represent a higher contrast. (B) Relative f_H period as a function of time for the animal shown in A. The relative f_H period is the period between two beats normalized by the average period obtained during the 10 s prior to the stimulation. (C) Mean relative f_H period as a function of time for the five stimuli (n=17, with shaded s.e.m.). (D) Normalized cardiac response to the five contrast stimuli. This variable is the area under the curve in B during the stimulation time, divided by the sum of the individual responses. The markers and bars represent the mean response and s.e.m. for each stimulus, and the light gray lines illustrate the individual responses. The dashed curve represents a second degree polynomial fit (see Results). (E) f_H recordings from a crab when confronted with the polarized stimuli 0, 22.5 and 45 deg (object e-vector: 82, 104.5 and 127 deg, respectively). In A–C and E, the black line under the plot illustrates the angular size of the looming object. The shaded area highlights the expansion of the object. (F) Normalized cardiac response (mean ±s.e.m.) to the different polarized stimuli. One group of animals was presented with the stimuli specified in E (n=13), another with the stimuli 45, 67.5 and 90 deg (object e-vector: 127, 149.5 and 172 deg, respectively, n=19). The light gray lines illustrate the individual responses. Comparisons were made between 0 and 22.5 deg versus 45 deg, and 67.5 and 90 deg versus 45 deg. Significant differences are indicated as follows: *P<0.05; ***P<0.0005.

from this result and two other studies (How et al., 2012, 2014), this theoretical model has not been validated sufficiently in the behavioral context of polarized object detection.

In the present study, we characterized the polarization contrast sensitivity of the grapsid crab *N. granulata* by studying its escape behavior and cardiac activity. As changes in escape behavior and heart rate have shown to be good indices of the stimulus intensity contrast (escape behavior: Oliva and Tomsic, 2012; cardiac activity: Fig. 4D), we assume that changes in these responses reflect the polarization contrast perceived by the animals. We found maximum changes in escape and heart rate when the e-vector from the object and the background were aligned with the vertical and horizontal. Conversely, when the orientation of one of these e-vectors was at 45 deg and the other at 135 deg, the animals produced minimum responses.

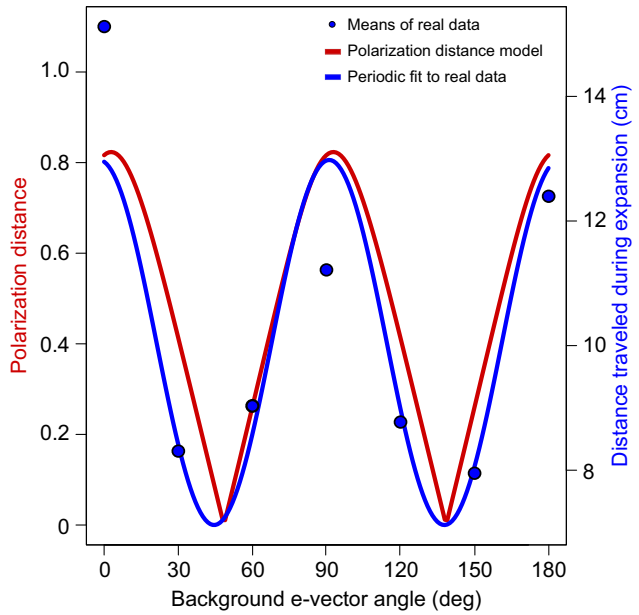

Fig. 5. Theoretical predictions for polarization contrast perception and experimental data. The red curve represents the polarization distance predicted by the theoretical model proposed by How and Marshall (2014). We fed the model with the polarization attributes of objects and backgrounds in the present work. The blue curve corresponds to the function estimated by fitting a periodic function to our experimental data. The blue circles represent the means of the behavioral data.

Fig. 5 shows the polarization distance calculated for a two-channel system, one vertical and the other horizontal, for the light parameters of the polarized objects and backgrounds used in this work (red curve, left y-axis; we used S_p=10, simulating a system with high polarization sensitivity according to How and Marshall, 2014). The mean distance traveled by the animals for the different polarization stimuli and the fitted curve were plotted in the same graph (blue markers and blue curve, respectively, right y-axis). Both curves are highly similar, supporting the idea that *N. granulata* uses a vertical and a horizontal channel to extract the polarization of light and compute polarization contrast similarly as predicted by the model. Moreover, we obtained behavioral and physiological results that provide strong empirical support for the model that estimates perceptual distances in object-based polarization vision.

One remarkable difference between color and polarization vision is that the latter is strongly dependent upon the relative orientation of the eye with respect to the environment it is sensing. At least in the lateral pole of the eye of decapod crustaceans, the microvilli of seven of eight retinular cells (R1–R7) are aligned parallel and perpendicular to the horizontal rows of the ommatidial facet array (Waterman, 1981; Alkaladi et al., 2013; Glantz, 2007). *Neohelice granulata* is a semi-terrestrial crab that inhabits the intertidal zone of estuaries and salt marshes (Spivak, 2010). These are coastal wetlands that produce horizontally polarized light reflections. Like other semi-terrestrial crabs inhabiting flat environments that also produce horizontally polarized backgrounds, *N. granulata* ends to keep its eyes in a stable position relative to the environment (Nalbach et al., 1989; Zeil, 1990; Land and Layne, 1995). Particularly, regardless of the posture or means of locomotion, the eyestalk of *N. granulata* keeps an inclination of 50 deg with respect to the horizontal plane (Berón de Astrada et al., 2012). This strategy has been related to animals inhabiting flat environments that would benefit from keeping the acute horizontal band (and the ommatidial facet array) of high vertical resolution of their eyes aligned with the horizon (Nalbach et al., 1989; Land and Layne, 1995; Zeil and Al-Mutairi, 1996). In addition, based on studies performed in cephalopods, Talbot and Marshall (2011) proposed that maintaining a stable state of the eye ensures maximum sensitivity or discriminability to horizontal and vertical e-vectors at all times. However, maximum contrast sensitivity for objects and background e-vectors aligned with the vertical and horizontal orientations had not been demonstrated before (but see How et al., 2012, 2014).

The maximization of polarization contrast sensitivity seems not to be restricted to animals that maintain their eyes stable relative to the outside world, but also occurs in animals that constantly scan their environment with highly active eye movements (Daly et al., 2016). This is the case for stomatopod crustaceans that only fix their eyes on scenes or objects of interest occasionally (Cronin et al., 1988; Land et al., 1990). Recently, it was shown that two species of stomatopods, *Gonodactylus smithii* and *Odontodactylus scyllarus*, rotate their eyes to align particular photoreceptors relative to the angle of polarization of a linearly polarized visual stimulus, maximizing the polarization contrast between an object of interest and its background (Daly et al., 2016). Moreover, dynamic maximization of polarization sensitivity seems not to be restricted to object-based polarization vision. In the context of navigation using sky polarization patterns, it has been observed that insects, such as the dung beetle *Scarabaeus rugosus* or desert ants, perform whole-body rotational movements to scan the sky (e.g. Byrne et al., 2003; Wehner, 1989). It has been suggested that such whole-body movements could be involved in modulating the polarization signals

received by the eyes, similarly to what is observed in object-based polarization vision in stomatopods (Daly et al., 2016).

Yet how is object-based polarization detection accomplished in the nervous system? Most of the physiological studies about polarization processing in crustaceans have been performed by Glantz and co-workers in the crayfish (reviewed in Glantz, 2001). At the two most peripheral stages of the visual system, the lamina and medulla externa neuropiles, four classes of visual interneurons exhibit polarization sensitivity: lamina monopolar cells, tangential cells, sustaining cells and dimming cells (Glantz, 1996a,b; Glantz and McIsaac, 1998). Sustaining and dimming dendrites innervate the medulla, where they collect information from a large number of visual columns and project to the midbrain. Based on the fact that the sustaining neurons present maximum responses to vertically polarized light while dimming neurons respond maximally to horizontally polarized light, Glantz proposed that these neurons form a two-channel polarization analyzer. However, none of the polarization-sensitive cells studied in crayfish are exclusively polarization sensitive. The information about polarization is confounded with the signals of intensity contrast throughout the system. A possible explanation of this result is that polarization sensitivity in the early stages of the visual pathway may enhance contrast where intensity differences are low (Leggett, 1976; Bernard and Wehner, 1977; Glantz, 2001).

In *N. granulata*, we have identified the polarization sensitive neurons described in crayfish (Berón de Astrada et al., 2001, 2009, 2013; Tomsic et al., 2003). At present, we have presented polarized stimuli just to sustaining and dimming cells (Berón de Astrada et al., 2009). In both crayfish and *N. granulata*, upon a light pulse, sustaining neurons increase the firing rate whereas dimming neurons reduce the firing rate, and the magnitude of these responses depends on the intensity of the light pulse. When presented with a rotating e-vector of polarized light, sustaining neurons show maximum depolarization when the e-vector approaches the vertical, while dimming neurons show maximal depolarization to near horizontal e-vector orientations. This result suggests a similar processing of polarization information between crabs and crayfish as far as the medulla level. Nevertheless, further studies need to be performed to understand how polarization information is processed in decapods with object-based polarization vision.

Acknowledgements
We thank Angel Vidal for technical assistance and Violeta Medan for critically reading the manuscript.

Competing interests
The authors declare no competing or financial interests.

Author contributions
Conceptualization: G.H., M.B.A.; Methodology: M.A.B., V.P.-S., G.H., M.B.A.; Software: M.A.B., V.P.-S.; Validation: G.H., M.B.A.; Formal analysis: M.A.B., V.P.-S., G.H.; Investigation: M.A.B., V.P.-S., G.H., M.B.A.; Data curation: M.A.B., G.H., M.B.A.; Writing - original draft: M.A.B., V.P.-S., M.B.; Writing - review & editing: M.A.B., V.P.-S., G.H., M.B.A.; Project administration: M.B.A.; Funding acquisition: M.B.A.

Funding
This study was supported by the Universidad de Buenos Aires (UBACYT 20020150100179BA to M.B.A.), the Consejo Nacional de Investigaciones Científicas y Técnicas (PIP11220130100379CO to M.B.A.) and the Agencia Nacional de Promoción Científica y Tecnológica (PICT 2012-1920 to M.B.A.).

References
Alkaladi, A., How, M. J. and Zeil, J. (2013). Systematic variations in microvilli banding patterns along fiddler crab rhabdoms. *J. Comp. Physiol. A* **199**, 99-113.
Beauchamp, R. D. and Rowe, J. S. (1977). Goldfish spectral sensitivity: a conditioned heart rate measure in restrained or curarized fish. *Vision Res.* **17**, 617-624.
Bengochea, M. (2017). Morphological and physiological characterization of columnar neurons projecting from the second to the third optic ganglion in arthropods. *PhD thesis*, University of Buenos Aires, Buenos Aires, Argentina.
Bernard, G. D. and Wehner, R. (1977). Functional similarities between polarization vision and color vision. *Vision Res.* **17**, 1019-1028.
Berón de Astrada, M., Sztarker, J. and Tomsic, D. (2001). Visual interneurons of the crab *Chasmagnathus* studied by intracellular recordings *in vivo*. *J. Comp. Physiol. A* **187**, 37-44.
Berón de Astrada, M., Tuthill, J. C. and Tomsic, D. (2009). Physiology and morphology of sustaining and dimming neurons of the crab *Chasmagnathus granulatus* (Brachyura: Grapsidae). *J. Comp. Physiol. A. Neuroethol. Sens. Neural. Behav. Physiol.* **195**, 791-798.
Berón de Astrada, M., Bengochea, M., Medan, V. and Tomsic, D. (2012). Regionalization in the eye of the grapsid crab *Neohelice granulata* (=*Chasmagnathus granulatus*): variation of resolution and facet diameters. *J. Comp. Physiol. A* **198**, 173-180.
Berón de Astrada, M., Bengochea, M., Sztarker, J., Delorenzi, A. and Tomsic, D. (2013). Behaviorally related neural plasticity in the arthropod optic lobes. *Curr. Biol.* **23**, 1389-1398.
Burnovicz, A., Oliva, D. and Hermitte, G. (2009). The cardiac response of the crab *Chasmagnathus granulatus* as an index of sensory perception. *J. Exp. Biol.* **212**, 313-324.
Byrne, M., Dacke, M., Nordström, P., Scholtz, C. and Warrant, E. (2003). Visual cues used by ball-rolling dung beetles for orientation. *J. Comp. Physiol. A* **189**, 411-418.
Cronin, T. W., Nair, J. and Doyle, D. (1988). Ocular tracking of rapidly moving visual targets by stomatopod crustaceans. *J. Exp. Biol.* **138**, 155-179.
Cronin, T. W., Johnsen, S., Marshall, J. and Warrant, E. J. (2014). *Visual Ecology*. Princeton, NJ: Princeton University Press.
Daly, I. M., How, M. J., Partridge, J. C., Temple, S. E., Marshall, N. J., Cronin, T. W. and Roberts, N. W. (2016). Dynamic polarization vision in mantis shrimps. *Nat. Commun.* **7**, 12140.
Glantz, R. M. (1996a). Polarization sensitivity in crayfish lamina monopolar neurons. *J. Comp. Physiol. A* **178**, 413-425.
Glantz, R. M. (1996b). Polarization sensitivity in the crayfish optic lobe: peripheral contributions to opponency and directionally selective motion detection. *J. Neurophysiol.* **76**, 3404-3414.
Glantz, R. M. (2001). Polarization analysis in the crayfish visual system. *J. Exp. Biol.* **204**, 2383-2390.
Glantz, R. M. (2007). The distribution of polarization sensitivity in the crayfish retinula. *J. Comp. Physiol. A* **193**, 893-901.
Glantz, R. M. and McIsaac, A. (1998). Two-channel polarization analyzer in the sustaining fiber-dimming fiber ensemble of crayfish visual system. *J. Neurophysiol.* **80**, 2571-2583.
Glantz, R. M. and Schroeter, J. P. (2006). Polarization contrast and motion detection. *J. Comp. Physiol. A* **192**, 905-914.
Grober, M. S. (1990). Luminescent flash avoidance in the nocturnal crab *Portunus xantusii*. I. The effects of luminescence and mechanical stimulation on heart rate. *J. Exp. Biol.* **148**, 415-426.
Hemmi, J. M. and Tomsic, D. (2012). The neuroethology of escape in crabs: from sensory ecology to neurons and back. *Curr. Opin. Neurobiol.* **22**, 194-200.
Horváth, G. and Varjú, D. (2004). *Polarized Light in Animal Vision*. Berlin: Springer-Verlag.
How, M. J. and Marshall, N. J. (2014). Polarization distance: a framework for modelling object detection by polarization vision systems. *Proc. Biol. Sci.* **281**, 20131632.
How, M. J., Pignatelli, V., Temple, S. E., Marshall, N. J. and Hemmi, J. M. (2012). High e-vector acuity in the polarisation vision system of the fiddler crab *Uca vomeris*. *J. Exp. Biol.* **215**, 2128-2134.
How, M. J., Christy, J., Roberts, N. W. and Marshall, N. J. (2014). Null point of discrimination in crustacean polarisation vision. *J. Exp. Biol.* **217**, 2462-2467.
How, M. J., Christy, J. H., Temple, S. E., Hemmi, J. M., Marshall, N. J. and Roberts, N. W. (2015). Target detection is enhanced by polarization vision in a fiddler crab. *Curr. Biol.* **25**, 3069-3073.
Johnsen, S. (2012). *The Optics of Life*. Princeton, NJ: Princeton University Press.
Johnsen, S., Marshall, N. J. and Widder, E. A. (2011). Polarization sensitivity as a contrast enhancer in pelagic predators: lessons from *in situ* polarization imaging of transparent zooplankton. *Philos. Trans. R Soc. Lond. B Biol. Sci.* **366**, 655-670.
King, A. J. and Adamo, S. A. (2006). The ventilatory, cardiac and behavioural responses of resting cuttlefish (*Sepia officinalis* L.) to sudden visual stimuli. *J. Exp. Biol.* **209**, 1101-1111.
Labhart, T. (2016). Can invertebrates see the e-vector of polarization as a separate modality of light? *J. Exp. Biol.* **219**, 3844-3856.
Land, M. and Layne, J. (1995). The visual control of behaviour in fiddler crabs. I. Resolution, thresholds and the role of the horizon. *J. Comp. Physiol. A* **177**, 81-90.
Land, M. F., Marshall, J. N., Brownless, D. and Cronin, T. W. (1990). The eye-movements of the mantis shrimp *Odontodactylus scyllarus* (Crustacea: Stomatopoda). *J. Comp. Physiol. A* **167**, 155-166.

Leggett, L. M. W. (1976). Polarised light-sensitive interneurones in a swimming crab. *Nature* **262**, 709-711.
Marshall, J. and Cronin, T. W. (2011). Polarisation vision. *Curr. Biol.* **21**, R101-R105.
Marshall, N., Cronin, T. and Wehling, M. F. (2011). New directions in the detection of polarized light. *Philos. Trans. R. Soc. B Biol. Sci.* **366**, 615-616.
Nalbach, H.-O., Nalbach, G. and Forzin, L. (1989). Visual control of eye-stalk orientation in crabs: vertical optokinetics, visual fixation of the horizon, and eye design. *J. Comp. Physiol. A* **165**, 577-587.
Oliva, D. (2010). Mechanisms of visual detection and avoidance of collision stimuli in a new experimental model: the crab *Chasmagnathus granulatus*. *PhD thesis*, University of Buenos Aires, Argentina.
Oliva, D. and Tomsic, D. (2012). Visuo-motor transformations involved in the escape response to looming stimuli in the crab *Neohelice* (*Chasmagnathus*) *granulata*. *J. Exp. Biol.* **215**, 3488-3500.
Oliva, D., Medan, V. and Tomsic, D. (2007). Escape behavior and neuronal responses to looming stimuli in the crab *Chasmagnathus granulatus* (Decapoda: *Grapsidae*). *J. Exp. Biol.* **210**, 865-880.
Pignatelli, V., Temple, S. E., Chiou, T.-H. Roberts, N. W., Collin, S. P. and Marshall, N. J. (2011). Behavioural relevance of polarization sensitivity as a target detection mechanism in cephalopods and fishes. *Philos. Trans. R. Soc. B Biol. Sci.* **366**, 734-741.
Roberts, N. W., Porter, M. L. and Cronin, T. W. (2011). The molecular basis of mechanisms underlying polarization vision. *Philos. Trans. R. Soc. B Biol. Sci.* **366**, 627-637.
Sakai, K., Turkay, M. and Yang, S. L. (2006). Revision of the *Helice/Chasmagnathus* complex (Crustacea: Decapoda: Brachyura). *Abh Senckenberg Naturforsch Ges.* **565**, 1-76.
Sand, O. and Karlsen, H. E. (1986). Detection of infrasound by the Atlantic cod. *J. Exp. Biol.* **125**, 197-204.
Shashar, N. and Cronin, T. W. (1996). Polarization contrast vision in octopus. *J. Exp. Biol.* **199**, 999-1004.
Shaw, S. R. (1969). Sense-cell structure and interspecies comparisons of polarized-light absorption in arthropod compound eyes. *Vision Res.* **9**, 1031-1040.
Spivak, E. D. (2010). The crab *Neohelice* (=*Chasmagnathus*) *granulata*: an emergent animal model from emergent countries. *Helgol. Mar. Res.* **64**, 149-154.
Stowe, S. (1980). Spectral sensitivity and retinal pigment movement in the crab *Leptograpsus variegatus* (Fabricius). *J. Exp. Biol.* **87**, 73-98.
Talbot, C. M. and Marshall, J. N. (2011). The retinal topography of three species of coleoid cephalopod: significance for perception of polarized light. *Philos. Trans. R. Soc. B Biol. Sci.* **366**, 724-733.
Temple, S. E., Pignatelli, V., Cook, T., How, M. J., Chiou, T.-H., Roberts, N. W. and Marshall, N. J. (2012). High-resolution polarisation vision in a cuttlefish. *Curr. Biol.* **22**, R121-R122.
Tomsic, D., Berón de Astrada, M. and Sztarker, J. (2003). Identification of individual neurons reflecting short- and long-term visual memory in an arthropodo. *J. Neurosci.* **23**, 8539-8546.
Tuthill, J. C. and Johnsen, S. (2006). Polarization sensitivity in the red swamp crayfish *Procambarus clarkii* enhances the detection of moving transparent objects. *J. Exp. Biol.* **209**, 1612-1616.
Waterman, T. H. (1981). Polarization sensitivity. In *Handbook of Sensory Physiology*, Vol. VII/6B (ed. H. Autrum), pp. 281-469. New York: Springer.
Waterman, T. H. and Fernández, H. R. (1970). E-vector and wavelength discrimination by retinular cells of the crayfish *Procambarus*. *Z. vergl. Physiol.* **68**, 154-174.
Waterman, T. H. and Horch, K. W. (1966). Mechanism of polarized light perception. *Science* **154**, 467-475.
Wehner, R. (1989). The Hymenopteran skylight compass: matched filtering and parallel coding. *J. Exp. Biol.* **146**, 63-85.
Wehner, R. (2001). Polarization vision: a uniform sensory capacity? *J. Exp. Biol.* **204**, 2589-2596.
Wehner, R. and Labhart, T. (2006). Polarization vision. In *Invertebrate Vision* (ed. E. J. Warrant and D.-E. Nilsson), pp. 291-348. Cambridge: Cambridge University Press.
Yang, M., Carbó Tano, M. and Hermitte, G. (2013). Picrotoxin but not bicuculline partially abolishes the cardio-inhibitory responses induced by visual stimulation in the crab *Neohelice granulata*. *Physiol. Behav.* **110-111**, 198-205.
Zeil, J. (1990). Substratum slope and the alignment of acute zones in semi-terrestrial crabs (*Ocypode ceratophthalmus*). *J. Exp. Biol.* **152**, 573-576.
Zeil, J. and Al-Mutairi, M. (1996). The variation of resolution and of ommatidial dimensions in the compound eyes of the fiddler crab *Uca lactea annulipes* (Ocypodidae, Brachyura, Decapoda). *J. Exp. Biol.* **199**, 1569-1577.